Interplay between cost and benefits triggers nontrivial vaccination uptake

Benjamin Steinegger,[1] Alessio Cardillo,[2,3] Paolo De Los Rios,[1] Jesús Gómez-Gardeñes,[4,3] and Alex Arenas[5]

[1] *Laboratory for Statistical Biophysics, École Polytechnique Fédérale de Lausanne (EPFL), CH-1015 Lausanne, Switzerland*
[2] *Institut Català de Paleoecologia Humana i Evolució Social (IPHES), E-43007 Tarragona, Spain*
[3] *GOTHAM Lab – Institute for Biocomputation and Physics of Complex Systems (BIFI), University of Zaragoza, E-50018 Zaragoza, Spain*
[4] *Department of Condensed Matter Physics, University of Zaragoza, E-50009 Zaragoza, Spain*
[5] *Department d'Enginyeria Informática i Matemátiques, Universitat Rovira i Virgili, E-43007 Tarragona, Spain*

(Dated: February 6, 2018)

The containment of epidemic spreading is a major challenge in science. Vaccination, whenever available, is the best way to prevent the spreading, because it eventually immunizes individuals. However, vaccines are not perfect, and total immunization is not guaranteed. Imperfect immunization has driven the emergence of anti-vaccine movements that totally alter the predictions about the epidemic incidence. Here, we propose a mathematically solvable mean-field vaccination model to mimic the spontaneous adoption of vaccines against influenza-like diseases, and the expected epidemic incidence. The results are in agreement with extensive Monte Carlo simulations of the epidemics and vaccination co-evolutionary processes. Interestingly, the results reveal a non-monotonic behavior on the vaccination coverage, that increases with the imperfection of the vaccine and after decreases. This apparent counterintuitive behavior is analyzed and understood from stability principles of the proposed mathematical model.

The quantitative study of diseases propagation has captured the attention of statistical physicists since long [1–3]. Specifically, this approach has shed light on many conundrums by considering the networked structure of contacts, their time-varying and multi-layer character, as well as the recurrent nature of mobility patterns [4–8]. Vaccination, whenever possible, is the most effective way to harness and prevent the spreading of a disease [9]. Under normal circumstances, the decision of getting vaccinated can be considered as an act of *cooperation*, since it bestows benefits on the whole population at the expenses of single individuals. Notwithstanding, we are recently witnessing the emergence of widespread anti-vaccine movements, which are mainly fueled by misconceptions and mischievous news about vaccines [10–16]. Scientists (including physicists) are devoting tremendous efforts in designing efficient immunization strategies [17] as well as shedding light on the mechanisms behind the deliberate decision of not getting vaccinated and their harmful consequences [18, 19].

Vaccination can be modeled as a strategy of a game. Under such premises, the evolution of vaccines' voluntary adoption can be investigated using the machinery of game theory [20, 21] and statistical physics [22, 23]. The first studies carried out on vaccination games use classical game theory, with single round games in which agents have perfect knowledge of their odds to get infected [24, 25]. In reality, however, individuals are not perfectly aware of the risk to get infected, and vaccination coverage may evolve in time as byproduct of personal experiences or imitation. Therefore, evolutionary game theory is the natural workbench to tackle the problem. The seminal works in this direction assumed the simultaneous evolution of vaccination and spreading dynamics [26–28]. A different approach was used in the case of seasonal influenza, by considering that the spreading process reaches its stationary state before vaccination games take place [29–32].

In this Letter, we introduce a mean-field framework to mimic the spontaneous adoption of vaccines against influenza-like diseases. Our model captures the essence of previous approaches to gauge, analytically, the risk of epidemic outbreaks. In particular, we use a minimal evolutionary vaccination game to infer the strategies adopted before an epidemic season. This, in turns, allows us to estimate the risk of future outbreaks by encapsulating agents' strategies into an epidemic model. We get analytical results and insightful conclusions from the analysis of this framework in well-mixed populations. More specifically, we unveil how the interplay between the probability of infection, vaccine effectiveness, and cost, gives rise to non-linear responses in vaccine uptake. Our analysis reveals a non-monotonic behavior on the vaccination coverage which, surprisingly, increases as the vaccine quality deteriorates. Such counterintuitive behavior is analyzed and understood from stability principles of the proposed mathematical model.

Let us consider a well-mixed population of N agents/individuals. We asume that this population has initially undergone a Susceptible-Infected-Recovered (SIR) disease spreading [2, 3]. To stay simple and keep the problem still analytically solvable, we set the disease incidence in such previous season equal to α. Such quantity is an input parameter of the model and acts as a proxy for the perception of infection risk, *e.g.* advised through the mass-media. After the first outbreak, the vaccination dynamics takes place. As a result, agents converge to the decision of vaccinating (V) or not (NV).

The resulting strategy is the outcome of the evolutionary dynamics (see below) given the previous incidence, α, infection probability, β, recovery cost, T, the cost of the vaccine, c, and its failure rate γ or, equivalently, its *effectiveness* $(1-\gamma)$. The corresponding vaccine coverage – given by the fraction of vaccinated agents y^* – is used as the input of a new SIR spreading process, having the same β and T. The results of the SIR dynamics allow us to estimate the total infection incidence, R_∞, as a function of the relevant parameters, especially α. The mathematical definition of α is the probability of infection, in the previous outbreak, of an agent without protection against the disease.

Vaccination dynamics consists of a repeatedly played two strategy game, in which agents either take the vaccine ($s = V$) or not ($s = NV$). Agents will decide according to: *(i)* the cost associated to uptaking the vaccine (c) and *(ii)* the recovery cost (T) weighted by the perceived risk of getting infected by a contact in a future outbreak. The latter risk depends on the previous incidence α, the infection rate β, and the vaccine effectivenesss $(1-\gamma)$. It is worth stressing that the vaccination cost should not be seen purely as a financial one. It also includes for example vaccine hesitancy [11, 12]. The payoffs associated to each of the four possible encounters between pairs of agents are:

$$\begin{cases} P_{\mathrm{V}\to\,\mathrm{V}} & = -c - \gamma^2\beta\alpha T \\ P_{\mathrm{V}\to\,\mathrm{NV}} & = -c - \gamma\beta\alpha T \\ P_{\mathrm{NV}\to\,\mathrm{V}} & = -\gamma\beta\alpha T \\ P_{\mathrm{NV}\to\,\mathrm{NV}} & = -\beta\alpha T \end{cases} . \tag{1}$$

Where $P_{s_1\to s_2}$ is the payoff accumulated by an agent with strategy s_1 when it meets another having strategy s_2 ($s_1, s_2 \in \{V, NV\}$). As explained above, the prefactors of the recovery cost (T) in Eq.(1) are modulated by the perceived risk of infection given the previous outbreak, encapsulated in α, and the probability that an individual playing with strategy s_1 is infected by another with strategy s_2.

The fitness of an agent i, π_i, is defined as the sum of payoffs accumulated across its pairwise interactions. Every agent i with strategy s_i chooses randomly another j, with strategy s_j, compares their fitness (π_i, π_j) and if $\pi_j > \pi_i$ adopts j's strategy with probability:

$$\Gamma_{s_j\to s_i} = \frac{\pi_j - \pi_i}{\max\limits_{\forall s_a,s_b,s_c,s_d\in\{V,NV\}} (P_{s_a\to s_b} - P_{s_c\to s_d})} . \tag{2}$$

The strategies of the agents are updated synchronously after each round of the game. Using the above update function, and assuming that agents are well-mixed, the mean outcome of the individual decisions follows the so-called *replicator equation* [20]:

$$\dot{y} = y\left(\langle\pi_V\rangle - \langle\pi\rangle\right), \tag{3}$$

where y is the fraction of vaccinated agents, $\langle\pi_V\rangle$ the average payoff of a vaccinated agent, and $\langle\pi\rangle$ the average payoff of the population. According to the payoffs in Eq.(1), the replicator equation reads:

$$\dot{y} = -y(1-y)\Big\{c - \beta\alpha T(1-\gamma)\Big[1-(1-\gamma)y\Big]\Big\} . \tag{4}$$

The above equation admits two trivial equilibrium points ($y_{eq} = 0$ and $y_{eq} = 1$), and a third, nontrivial, one:

$$y^* = \frac{1}{1-\gamma}\left[1 - \frac{c}{\beta T\alpha(1-\gamma)}\right] . \tag{5}$$

The criteria for the existence of the latter equilibrium point has an intuitive interpretation. In fact, the condition $y^* > 0$ is equivalent to $P_{\mathrm{NV}\to\,\mathrm{NV}} < P_{\mathrm{V}\to\,\mathrm{NV}}$, which translates into a vaccination threshold for the transmission probability as $\tilde{\beta} = c/\alpha T(1-\gamma)$ [33]. In other words, it is impossible to observe vaccination in a system where $c > T$, *i.e.* where vaccinating costs more than recovery. The criteria $y^* < 1$ translates, instead, into $P_{\mathrm{V}\to\,\mathrm{V}} < P_{\mathrm{NV}\to\,\mathrm{V}}$, corresponding to $\beta < \tilde{\beta}/\gamma$. If this condition is not fulfilled, a vaccinated agent has a payoff higher than a non vaccinated one regardless of the opponents strategies, hence leading to full vaccination.

The stability analysis of the fixed points in Eq. (4) reveals that the monomorphic states, $y = 0$ and $y = 1$, respectively, are unstable in the presence of the internal fixed point, y^*, while the latter is stable [33]. In the absence of the internal fixed point, one of the two monomorphic states becomes stable while the other one stays unstable depending on whether $y^* < 0$ or $y^* > 1$. Therefore, for $\tilde{\beta} \le \beta \le \tilde{\beta}/\gamma$ the vaccination coverage, y_{eq}, is given by the internal fixed point $y_{eq} = y^*$, whereas for $\beta < \tilde{\beta}$ and $\tilde{\beta}/\gamma < \beta$ it is given by $y_{eq} = 0$ and $y_{eq} = 1$, respectively.

According to Eq. (5), high values of c are detrimental for vaccination, while high values of T and β boosts it. Additionally, the vaccination coverage depends exclusively on the ratio between vaccination and recovery costs, which we denote as $f = c/T$. Additionally, considering Eq. (5), one can see that full vaccination cannot be stable for a perfect vaccine unless $f = 0$.

More subtle is the dependence on the vaccination quality γ. In fact, lowering vaccine quality increases vaccine coverage ($dy^*/d\gamma > 0$) if the fraction of effectively vaccinated agents $y_{\mathrm{eff}} > 0.5$, where $y_{\mathrm{eff}} = (1-\gamma)y$. Noteworthy, albeit the quality of the vaccine worsens, agents will choose more often to vaccinate.

At first glance, the increase in vaccine uptake as its effectiveness decrease may seem counterintuitive. The rationale behind this is as follows: as γ increases there is a competition between the increasing risk of getting infected and the reduced protection bestowed by the vaccine itself, as shown in Fig. 1. To shed light on such competition, one may look at the decrease of the vac-

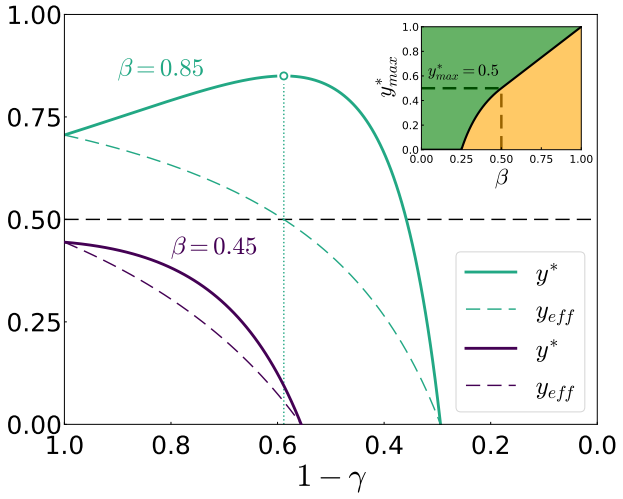

FIG. 1. Vaccination coverage at equilibrium, y^*, as a function of effectiveness, $1-\gamma$ for two different values of the infection probability β. The dashed line indicates the fraction of effectively vaccinated agents. The other parameters are $\alpha = 0.4$, $c = 0.1$, and $T = 1.0$. The maximum coverage $y^*_{\max}$ is denoted by a point and the dotted line delimits the tolerance range. The inset displays the value of the maximum coverage $y^*_{\max}$ as a function of infectivity β. The color highlights the region where vaccination takes place or not.

cine's effectiveness $1-\gamma$ as a dynamical process. As effectiveness decreases, the risk for a not vaccinated agent of getting infected by a previously vaccinated one becomes $y_{\text{eff}} \times \beta\alpha\gamma$. Conversely, the risk of a vaccinated agent to get infected by a non vaccinated becomes $(1-y_{\text{eff}}) \times \beta\alpha\gamma$. Comparing these two risks, the vaccinated agent has an advantage over the non vaccinated if $y_{\text{eff}} > (1 - y_{\text{eff}})$, which translates into $y_{\text{eff}} > 0.5$. Hence, the counterintuitive act of vaccinating when the efficiency of the vaccine is low, turns out to be a rational decision to mitigate the infection pressure. Moreover, the existence – for each infectivity β – of a maximum fraction of vaccinated agents, $y^*_{\max}$, delimitates a region of "tolerable effectiveness" beyond which agents decide to non vaccinate. Also, the position of $y^*_{\max}$ versus β splits the phase space into two distinct regions (Fig. 1 inset). Interestingly, this effect has been observed previously in other coevolutionary models [31, 32, 34], but never explained hitherto. At variance with y, the fraction of *effectively* vaccinated agents, y_{eff}, is always lowered by a decrease of the vaccine quality, *i.e.* $\frac{d((1-\gamma)y^*)}{d\gamma} < 0$. Therefore, the higher vaccination coverage is not counterbalancing the lower vaccine quality. The vaccine quality maximizing the vaccination coverage [33] is given by $dy^*/d\gamma = 0$, leading to $\gamma_c = 1 - \frac{2f}{\beta\alpha}$.

After discussing the outcome of the vaccination dynamics, we now turn our focus towards its impact on the subsequent epidemic outbreak. Assuming that the vaccination dynamics always ends up in one of its equilibrium points y_{eq}; we can use such information to compute the extent of a future epidemic outbreak by using a SIR compartmental model [3]. The dynamics of the SIR model is then given by:

$$\begin{cases} \dot{S} = -\beta IS \\ \dot{I} = \beta IS - \mu I \\ \dot{R} = \mu I \end{cases}, \tag{6}$$

where S, I, and R denote the fraction of susceptible, infected and recovered agents, respectively. The aforementioned quantities fulfill the conservation law $S + I + R + (1-\gamma)y_{\text{eq}} = 1$. Note that $\mu = 1/T$ indicates the recovery probability in agreement with the vaccination game. The fraction of recovered agents after the epidemics dies out, R_∞, is given by the following trascendental equation [33]:

$$R_\infty = 1 - (1-\gamma)y_{\text{eq}} - \left[1 - (1-\gamma)y_{\text{eq}} - I_0\right] e^{-\frac{\beta}{\mu} R_\infty}, \tag{7}$$

where I_0 is the initial fraction of infected agents. Eq. (7) has no analytical solution, hence it must be solved numerically. Nevertheless, in an infinite size system ($N \to \infty$), the term I_0 can be neglected since $I_0 \ll 1$. Thus, a non negligible fraction of recovered agents, R_∞, exists only if:

$$\beta > \frac{\mu}{1 - (1-\gamma)y_{\text{eq}}} = \beta_c \tag{8}$$

where β_c denotes the epidemic threshold. As expected, if the system displays no vaccination, $y_{\text{eq}} = 0$, and the above criteria reduces to the purely epidemic SIR threshold $\beta_c = \mu$. Instead, for the full vaccination case, $y_{\text{eq}} = 1$, the criteria becomes $\beta_c = \mu/\gamma$. Finally, for the internal fixed point, $y_{\text{eq}} = y^*$, the existence of $R_\infty > 0$ in Eq.(7) implies:

$$\frac{f}{\mu\alpha(1-\gamma)} > 1\,. \tag{9}$$

Surprisingly, this condition is independent of β. Therefore, the increased vaccination coverage balances the increased transmission probability in the subsequent epidemic outbreak.

In Fig. 2, we display the vaccination coverage, y_{eq} (panel a), and the fraction of recovered agents, R_∞ (panel b), as a function of the previous season incidence α, and the probability of infection β in the case of a perfect vaccine ($\gamma = 0$). As expected, a remarkably high fraction of recovered agents is observed for a highly infective epidemic (large β) paired with a small fraction of infected agents in the previous outbreak (small α). In (panel b), one can observe that, given a value of α, the fraction of recovered individuals is maximal at the vaccination threshold $\tilde{\beta}$. Actually, in an infinite system, the transcendental equation Eq. (7) takes three different forms

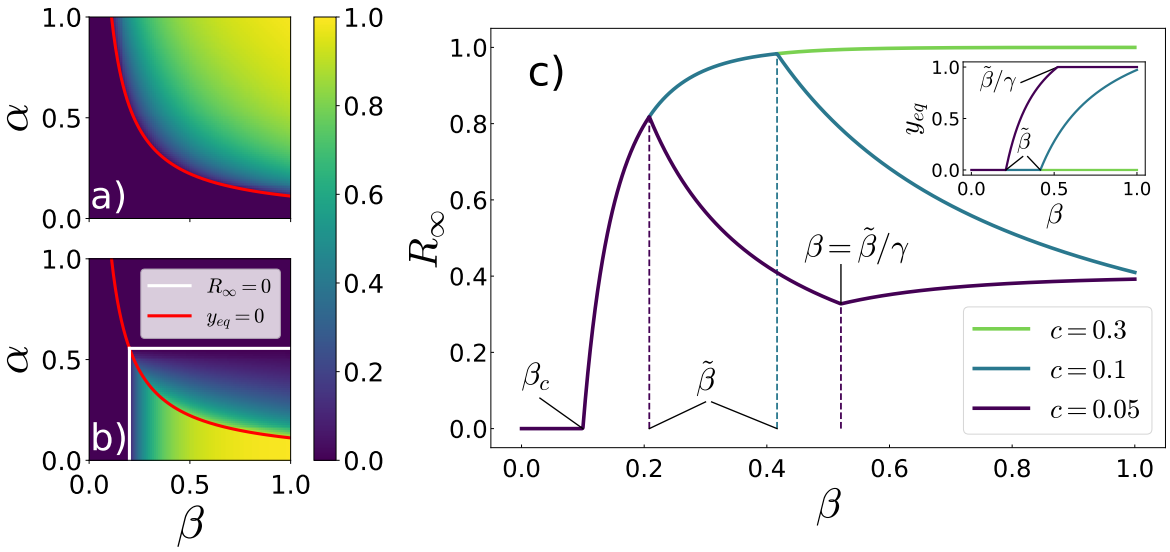

FIG. 2. Vaccination coverage, $y_{\rm eq}$, **(panel a)** and fraction of recovered individuals, R_∞, **(panel b)** as a function of disease incidence in the previous season, α, and infection probability, β. The red solid line corresponds to the vaccination threshold, $\tilde{\beta}$, separating the region where no vaccine uptake occurs from the one where nonzero vaccination could be observed. In (panel b), the white solid lines correspond to the epidemic thresholds in the absence of ($\beta = 0.2$), and in presence ($\alpha = 0.5$) of vaccination according to Eq. (8). The other variables are fixed to $c = 0.1$, $T = 1.0$, $\gamma = 0.1$ and $\mu = 0.2$. **(panel c)** R_∞ as a function of β for different costs of the vaccine, c. The inset presents the vaccination coverage. Additionally, the critical values of β are presented following Eq.(10) such as the purely epidemic threshold, β_c, the vaccination threshold, $\tilde{\beta}$, and the threshold for full vaccination, $\tilde{\beta}/\gamma$. The remaining variables are fixed to $T = 1.0$, $\gamma = 0.4$, $\alpha = 0.4$ and $\mu = 0.1$.

depending on the vaccination coverage:

$$\begin{cases} R_\infty = 1 - \mathrm{e}^{-\frac{\beta}{\mu} R_\infty} & \text{if} \quad \mu < \beta < \tilde{\beta} \\ R_\infty = \frac{\tilde{\beta}}{\beta}\left(1 - \mathrm{e}^{-\frac{\beta}{\mu} R_\infty}\right) & \text{if} \quad \tilde{\beta} \leqslant \beta < \frac{\tilde{\beta}}{\gamma} \\ R_\infty = \gamma\left(1 - \mathrm{e}^{-\frac{\beta}{\mu} R_\infty}\right) & \text{if} \quad \frac{\tilde{\beta}}{\gamma} \leqslant \beta \leqslant 1 \end{cases} . \qquad (10)$$

Using these equations, one can show that in the absence of the internal fixed point ($\beta < \tilde{\beta}$ and $\beta > \tilde{\beta}/\gamma$) $\frac{dR_\infty}{d\beta} > 0$. However, this is somehow expected since within such regimes vaccination coverage is constant ($y_{\rm eq} = 0$ or 1, respectively). Therefore, increasing the transmission probability β necessarily increases the fraction of recovered agents R_∞. In the intermediate regime $\tilde{\beta} < \beta < \tilde{\beta}/\gamma$ though, where the internal fixed point exists, one can show that $\frac{dR_\infty}{d\beta} < 0$. Consequently, vaccination emerges in a way such that it outweighs the increased transmission probability and hinders the epidemic spreading. The situation is illustrated in Fig.2.c. Therefore, the fraction of recovered agents R_∞ is locally maximal when vaccination emerges at $\beta = \tilde{\beta}$ and locally minimal when full vaccination is first reached at $\beta = \tilde{\beta}/\gamma$. The numerical exploration of the parameter space has confirmed hitherto that the global maximum is located at β_c. Moreover, the highest fraction of recovered, $R_\infty^{\max}$, for a fully vaccinated population ($y_{\rm eq} = 1$) corresponds to meaningless values of the parameters. To validate that the previous equations are actually describing the behavior of the considered system, we have compared the analytical results discussed above with those obtained via Monte Carlo simulations [33]. The agreement between analytical and numerical simulations, σ, is $\sim 2\%$.

Preliminary analysis show similar results to those presented in the current manuscript in complex networks, although we still do not have analytical solutions in such case. Notwithstanding, the well-mixed population proves to be a good approximation for the vaccination dynamics on networks. This is very likely due to the vaccination cost term in the total payoff, which does not scale with the degree of nodes. Additionally, the nontrivial increase in vaccine uptake – as effectiveness decreases – is also observed in simulations on networked populations [31].

Summing up, we have presented a mean-field model to predict vaccine uptake for influenza-like diseases using the disease incidence during previous outbreak season as a proxy for the "perception of infection risk." The model predicts the existence of a tolerance range of vaccine effectiveness, where a nontrivial increase in vaccination coverage takes place as the vaccine inefficiency increases. Albeit appearing irrational and counterintuitive at first sight, such behavior is – instead – due to the interplay between the vaccination game and the disease spreading processes. The model predicts also that highly infective – but under control – epidemics might prove dangerous for future infections, since they alter the "risk perception" of the agents, and induce them to non vaccination. Finally, as mentioned in the introduction, the time scale

between the two dynamics (decision and spreading) has always been considered fixed. The sole exception, up to our knowledge, are childhood diseases with long term immunity [27, 35]. The framework presented here could be used to fill the gap among different model formulations and unify them.

PDLR acknowledges the financial support of Swiss National Science Foundation under Grant No. CRSII2_147609. AC acknowledges the financial support of MINECO through Grant RYC-2012-01043. JGG acknowledges financial support from MINECO (projects FIS2015-71582-C2 and 377 FIS2014-55867-P) and from the Departamento de Industria e Innovación del Gobierno de Aragón y Fondo Social Europeo (FENOL group E-19). AA acknowledges financial support from Spanish MINECO (grant FIS2015-71582-C2-1), Generalitat de Catalunya ICREA Academia, and the James S. McDonnell Foundation.

[1] R. Pastor-Satorras, C. Castellano, P. Van Mieghem, and A. Vespignani, Epidemic processes in complex networks. Reviews of Modern Physics, **87**, 925–979 (2015).
[2] R. M. Anderson, and R. M. May, Population biology of infectious diseases: Part I. Nature **280**, 361–367 (1979).
[3] R. M. Anderson, and R. M. May, Infectious Diseases of Humans. Oxford University Press, (1992).
[4] R. Pastor-Satorras, and A. Vespignani, Epidemic Spreading in Scale-Free Networks. Physical Review Letters, **86**, 3200–3203 (2001).
[5] A. Vazquez, B. Rácz, A. Lukács, and A.-L. Barabási, Impact of Non-Poissonian Activity Patterns on Spreading Processes. Physical Review Letters, **98**, 158702 (2007).
[6] M. De Domenico, C. Granell, M. A. Porter, and A. Arenas, The physics of spreading processes in multilayer networks. Nature Physics, **12**, 901–906 (2016).
[7] P. Holme, Three faces of node importance in network epidemiology: Exact results for small graphs. Physical Review E, **96**, 62305 (2017).
[8] J. Gómez-Gardeñes, D. Soriano-Paños, and A. Arenas, Critical regimes driven by recurrent mobility patterns of reaction?diffusion processes in networks. Nature Phys. doi:10.1038/s41567-017-0022-7 (2018).
[9] M. Wadman, and J. You, The vaccine wars. Science, **356**, 364–365 (2017).
[10] On the wrong side of history. Nature Microbiology, **2**, 17046 (2017).
[11] P. Schmid, D. Rauber, C. Betsch, G. Lidolt, and M. -L. Denker, Barriers of Influenza Vaccination Intention and Behavior – A Systematic Review of Influenza Vaccine Hesitancy, 2005 – 2016. PLoS ONE, **12**, e0170550 (2017).
[12] H. J. Larson, C. Jarrett, E. Eckersberger, D. M. D. Smith, and P. Paterson, Understanding vaccine hesitancy around vaccines and vaccination from a global perspective: A systematic review of published literature, 2007–2012. Vaccine, **32**, 2150–2159 (2014).
[13] A. Wakefield, *et al.* RETRACTED: Ileal-lymphoid-nodular hyperplasia, non-specific colitis, and pervasive developmental disorder in children. The Lancet, **351**, 637–641 (1998).
[14] D. A. Salmon, L. H. Moulton, S. B. Omer, M. P. deHart, S. Stokley, and N. A. Halsey, Factors Associated With Refusal of Childhood Vaccines Among Parents of School-aged Children: A Case-Control Study. Arch. Pediatr. Adolesc. Med. **159**, 470–476 (2005).
[15] E. K. Brunson, The impact of social networks on parents' vaccination decisions. Pediatrics **131**, e1397-404 (2013).
[16] G. L. Freed, S. J. Clark, A. T. Butchart, D. C. Singer, and M. M. Davis, Sources and perceived credibility of vaccine-safety information for parents. Pediatrics **127**, 107–12 (2011).
[17] Z. Wang *et al.* Statistical physics of vaccination. Physics Reports, **664**, 1–113 (2016).
[18] C. Betsch, Advocating for vaccination in a climate of science denial. Nature Microbiology, **2**, 17106 (2017).
[19] C. Betsch, R. Böhm, L. Korn, and C. Holtmann, On the benefits of explaining herd immunity in vaccine advocacy. Nature Human Behaviour, **1**, 56 (2017).
[20] M. A. Nowak, Evolutionary Dynamics – Exploring the Equations of Life. Belknap Press of Harvard University Press, (2006).
[21] H. Gintis, Game Theory Evolving (2nd ed.). Princeton University Press, (2009). ISBN:9780691140513
[22] C. Hauert and G. Szabó, Game theory and physics, American Journal of Physics, **73 (5)**, 405–414 (2005)
[23] M. Perc and A. Szolnoki, Coevolutionary games – A mini review, Biosystems, **99 (2)**, 109–125 (2010)
[24] C. T. Bauch, A. P. Galvani, and D. J. D. Earn, Group interest versus self-interest in smallpox vaccination policy. Proceedings of the National Academy of Sciences of USA, **100**, 10564–10567 (2003).
[25] C. T. Bauch, and D. J. D. Earn, Vaccination and the theory of games. Proceedings of the National Academy of Sciences of USA, **101**, 13391–13394 (2004).
[26] S. Bhattacharyya, C. T. Bauch, A game dynamic model for delayer strategies in vaccinating behaviour for pediatric infectious diseases. Journal of Theoretical Biology, **267**, 276–282 (2010).
[27] C. T. Bauch, S. Bhattacharyya, Evolutionary Game Theory and Social Learning Can Determine How Vaccine Scares Unfold. PLoS Computational Biology **8**, e1002452 (2012).
[28] A. dOnofrio, P. Manfredi, and P. Poletti, The Interplay of Public Intervention and Private Choices in Determining the Outcome of Vaccination Programmes. PLoS ONE **7**, e45653 (2012).
[29] F. Fu, R. I. Rosenbloom, L. Wang, and M, A. Nowak, Imitation dynamics of vaccination behaviour on social networks. Proceedings of the Royal Society B: Biological Sciences, **278**, 42–49 (2011).
[30] H. Zhang, F. Fu, W. Zhang, and B. Wang, Rational behavior is a "double-edged sword" when considering voluntary vaccination. Physica A: Statistical Mechanics and its Applications **391**, 4807–4815 (2012).
[31] A. Cardillo, C. Reyes-Suárez, F. Naranjo, and J. Gómez-Gardeñes. Evolutionary vaccination dilemma in complex networks. Physical Review E, **88**, 32803 (2013).
[32] B. Wu, F. Fu, and L. Wang. Imperfect Vaccine Aggravates the Long-Standing Dilemma of Voluntary Vaccination. PLoS ONE, **6**, e20577 (2011).
[33] See supplemental material.
[34] L. G. Alvarez-Zuzek, C. E. La Rocca, J. R. Iglesias, and L. A. Braunstein, Epidemic spreading in multiplex net-

works influenced by opinion exchanges on vaccination. PLoS ONE, **12**, e0186492 (2017).

[35] C. T- Bauch, Imitation dynamics predict vaccinating behaviour. Proc. R. Soc. B **272**, 1669–1675 (2005).

Supplemental Information: Interplay among cost and benefits triggers nontrivial vaccination uptake

STABILITY OF THE FIXED POINTS

The evolution of the fraction of vaccinated agents is governed by the replicator equation as presented in Eq. (4). For analyzing the stability of the fixed points, we need to consider the derivative of the RHS of Eq. (4), i.e. of the selection gradient $F(y)$:

$$\frac{dF(y)}{dy} = -(1-2y)\left[c - \beta\alpha T(1-\gamma)(1-(1-\gamma)y)\right] - y(1-y)\beta\alpha T(1-\gamma)^2 \tag{S1}$$

Evaluating the derivative at the internal fixed point,y^*, we get:

$$\left.\frac{dF(y)}{dy}\right|_{y=y^*} = -y^*(1-y^*)\beta\alpha T(1-\gamma)^2 \tag{S2}$$

Therefore, if the internal fixed point is present ($0 < y^* < 1$), it is stable, since $\left.\frac{dF(y)}{dy}\right|_{y=y^*} < 0$. Additionally, one can see that if $y^* < 0$ or $y^* > 1$, the fixed point y^* is unstable. Evaluating now the derivative at the monomorphic states, we get:

$$\begin{cases} \left.\frac{dF(y)}{dy}\right|_{y=0} & = \beta\alpha T(1-\gamma) - c = P_{\text{V}\,\to\,\text{NV}} - P_{\text{NV}\,\to\,\text{NV}} \\ \left.\frac{dF(y)}{dy}\right|_{y=1} & = c - \beta\alpha T(1-\gamma)\gamma = P_{\text{NV}\,\to\,\text{V}} - P_{\text{V}\,\to\,\text{V}} \end{cases} \tag{S3}$$

As stressed in the main text, the conditions $y^* > 0$ and $y^* < 1$ translate as $P_{\text{V}\,\to\,\text{NV}} - P_{\text{NV}\,\to\,\text{NV}}$ and $P_{\text{NV}\,\to\,\text{V}} - P_{\text{V}\,\to\,\text{V}}$, respectively. Therefore, considering Eq. (S3), the monomorphic states are unstable in the presence of the internal fixed point. In contrast, in the absence of the internal fixed point, $y = 0$ will become stable if $y^* < 0$ while $y = 1$ stays unstable and vice versa for $y^* > 1$. Figure S1 presents the selection gradient as a function of the vaccination coverage, y, in the presence of the internal fixed point, y^*. One can see that y^* is stable and as the internal fixed point is shifted to $y^* = 0$ or $y^* = 1$ the corresponding monomorphic state reaches stability.

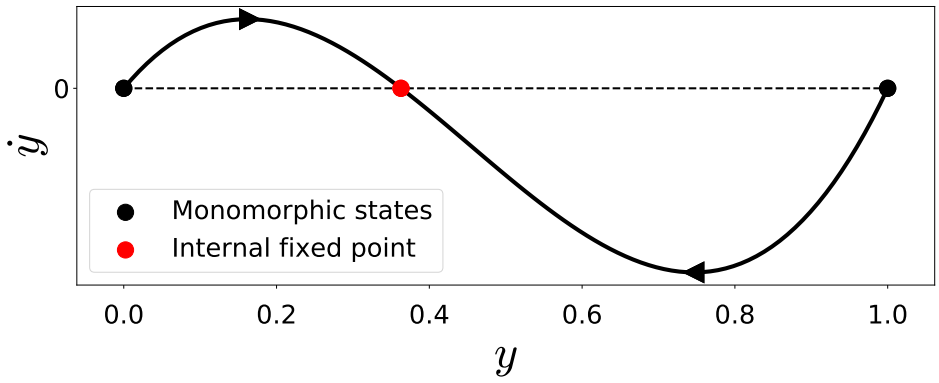

FIG. S1. Selection gradient, $\dot{y} = \mathrm{F(y)}$, as a function of the vaccination coverage, y. The parameters are set to $c = 0.1$, $\alpha = 0.3$, $\beta = 0.55$, $\gamma = 0.1$ and $T = 1.0$.

DEPENDENCE OF THE VACCINATION UPTAKE ON VACCINE QUALITY γ

The relation between the fraction of vaccinated individuals at equilibrium, y^*, and the quality of the vaccine, γ presented in Eq. (5) of the main text is not trivial. In particular, $dy^*/d\gamma > 0$ if $(1-\gamma)y^* = y_{eff} > 0.5$. Consequently, there are three different regimes depending on γ. The first one is the absence of vaccination independently of γ, corresponding to $\beta < \frac{c}{\alpha T} = \frac{f}{\alpha}$. In the second regime $y^*(\gamma = 0) < 0.5$ the vaccination coverage is monotonously decreasing with γ. Therefore, maximal vaccination coverage is reached for a perfect vaccine $\gamma = 0$, which is equivalent to $\beta \leq \frac{2f}{\alpha}$. In the third regime $\beta > \frac{2f}{\alpha}$, the dependence of y^* on γ is non monotonous, wherefore the vaccination coverage is maximal for a non perfect vaccine. The vaccine quality maximizing the vaccination coverage is then found from $dy^*/d\gamma = 0$, leading to:

$$\gamma_c = 1 - \frac{2f}{\beta\alpha}\,. \tag{S4}$$

The vaccine quality, which is maximizing the vaccination coverage can also be seen as a tolerance threshold. If $1-\gamma$ becomes worse than $1-\gamma_c$, agents start refusing taking the vaccine and the vaccination coverage drops, as illustrated in Fig. S2. From there, the maximal vaccination coverage in the three regimes is then given by:

$$\begin{cases} y^*_{max} = 0 & \text{if } \beta < \frac{f}{\alpha} \\ y^*_{max} = 1 - \frac{f}{\beta\alpha} & \text{if } \frac{f}{\alpha} < \beta < \frac{2f}{\alpha} \\ y^*_{max} = \frac{\beta\alpha}{4f} & \text{if } \frac{2f}{\alpha} < \beta\,. \end{cases} \tag{S5}$$

These relations have been presented in the inset of Fig. 1. One can see in this figure as well in Eq. (S5) that at the critical point $\beta = \frac{f}{\alpha}$ the derivative of y^*_{max} with respect to β has a discontinuity, whereas at the critical point $\beta = \frac{2f}{\alpha}$ the derivative of y^*_{max} with respect to β is continuous.

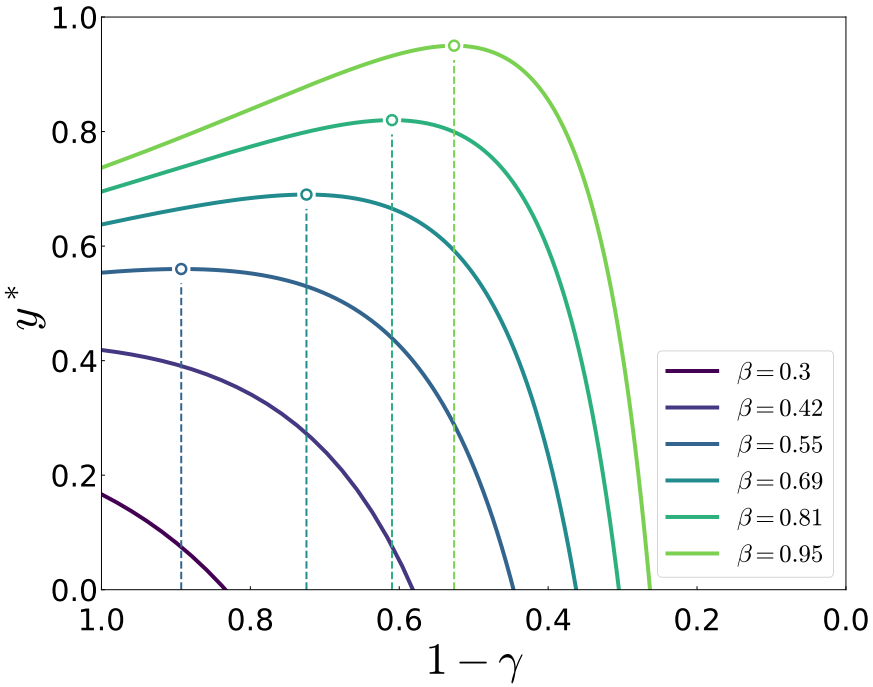

FIG. S2. Fraction of vaccinated agents, y^*, as a function of the vaccine efficiency, $1-\gamma$, for various values of the transmission probability, β. The other parameters are set to $c = 0.1$, $\alpha = 0.4$, $\mu = 0.1$ and $T = 1.0$. The point on each curve indicates the position of $y^*_{max}(\beta)$ and the corresponding value of $1-\gamma$.

EXTREMAL VALUES OF R_∞

In Fig. 2 of the main manuscript, we have displayed the behavior of R_∞ versus β for different values of cost c. For certain values of the latter, the R_∞ curve has a local maximum at $\beta = \beta_c$, and a local minimum for $\tilde{\beta}/\gamma$. This section is devoted to the calculation of such values. In particular, we compute the derivative of R_∞ with respect to β, $\frac{dR_\infty}{d\beta}$. By performing such operation on both sides of Eq. (10), we get:

$$\begin{cases} \dfrac{dR_\infty}{d\beta} = \dfrac{R_\infty}{\mu\left(\mathrm{e}^{\frac{\beta}{\mu}R_\infty} - \dfrac{\beta}{\mu}\right)} & , \text{ if } \mu < \beta < \tilde{\beta} \\ \dfrac{dR_\infty}{d\beta} = \dfrac{R_\infty + \dfrac{\mu}{\beta}\left(1 - \mathrm{e}^{\frac{\beta}{\mu}R_\infty}\right)}{\dfrac{\mu\beta}{\tilde{\beta}}\left(\mathrm{e}^{\frac{\beta}{\mu}R_\infty} - \dfrac{\tilde{\beta}}{\mu}\right)} & , \text{ if } \tilde{\beta} < \beta < \frac{\tilde{\beta}}{\gamma} \\ \dfrac{dR_\infty}{d\beta} = \dfrac{R_\infty\gamma}{\mu\left(\mathrm{e}^{\frac{\beta}{\mu}R_\infty} - \gamma\dfrac{\beta}{\mu}\right)} & , \text{ if } \frac{\tilde{\beta}}{\gamma} < \beta < 1\,. \end{cases} \tag{S6}$$

To infer information about the sign of $\frac{dR_\infty}{d\beta}$ we need to bound R_∞. In fact, by using again Eq. (10) and the inequality $1 - \mathrm{e}^{-x} > \frac{x}{1+x}$, we find a lower bound for R_∞ as:

$$\begin{cases} R_\infty > 1 - \frac{\mu}{\beta} & , \text{ if } \mu < \beta < \tilde{\beta} \\ R_\infty > \frac{\tilde{\beta}}{\beta} - \frac{\mu}{\beta} & , \text{ if } \tilde{\beta} < \beta < \frac{\tilde{\beta}}{\gamma} \\ R_\infty > \frac{\tilde{\beta}}{\beta} - \frac{\mu}{\beta} & , \text{ if } \frac{\tilde{\beta}}{\gamma} < \beta < 1\,. \end{cases} \tag{S7}$$

These lower bounds can then be combined with the inequality $\mathrm{e}^{\frac{\lambda}{\mu}R_\infty} \geq 1 + \frac{\lambda}{\mu}R_\infty$. The strict inequality holds for all $R_\infty > 0$. This enables us to develop the expressions for the derivative in Eq. (S6), leading to:

$$\begin{cases} \frac{dR_\infty}{d\beta} > 0 & , \text{ if } \mu < \beta < \tilde{\beta} \\ \frac{dR_\infty}{d\beta} < 0 & , \text{ if} \\ tilde\beta < \beta < \frac{\tilde{\beta}}{\gamma} & \\ \frac{dR_\infty}{d\beta} > 0 & , \text{ if } \frac{\tilde{\beta}}{\gamma} < \beta < 1\,. \end{cases} \tag{S8}$$

The cases $\beta < \tilde{\beta}$ and $\frac{\tilde{\beta}}{\gamma} < \beta$ are trivial. In these regimes the vaccination coverage does not vary with β ($y_{eq} = 0$ and $y_{eq} = 1$, respectively). Consequently, R_∞ increases monotonously with β. On the other hand, as already mentioned in the main text, intermediate values of β trigger vaccination which counterbalances the increase of β, thus reducing R_∞. From there we conclude that the fraction of recovered agents is locally maximal at $\beta = \tilde{\beta}$ and locally minimal at $\beta = \tilde{\beta}/\gamma$. Since we do not have an explicit expression for R_∞ it was not possible to prove that the local maximum at $\beta = \tilde{\beta}$ is also a global one. However, the numerical exploration of the parameter space have not pinpointed any case in which global and local maximum do not coincide. Also, having the maximal fraction of infected agents in a fully vaccinated configuration would require an unphysical choice of the parameters. In the case $\tilde{\beta}/\gamma > 1$, the system will never be in the third regime. Consequently, R_∞ monotonously decreases once vaccination emerges. Similarly, one might have $\tilde{\beta} > 1$ in which case the system shows no vaccination and R_∞ monotonously increases with β.

DETAILS ABOUT MONTE CARLO SIMULATIONS

In the main text, we compared the macroscopic behavior of the model using Monte Carlo simulations. Here, we provide the details concerning the simulation framework. The simulations have been made for a system of $N = 1000$ agents updating their strategy accordingly to Eq. (2), and averaged over $N_{real} = 50$ realizations. The difference between theory and the simulation for the vaccine coverage, y, and fraction of infected agents, R_∞, is plotted in panels a and b of Fig. S3.

The maximal difference for y and R_∞ are around 0.2% an 2.5%, respectively. The average relative errors, instead, are 0.2% for V and 2.0% for R_∞.

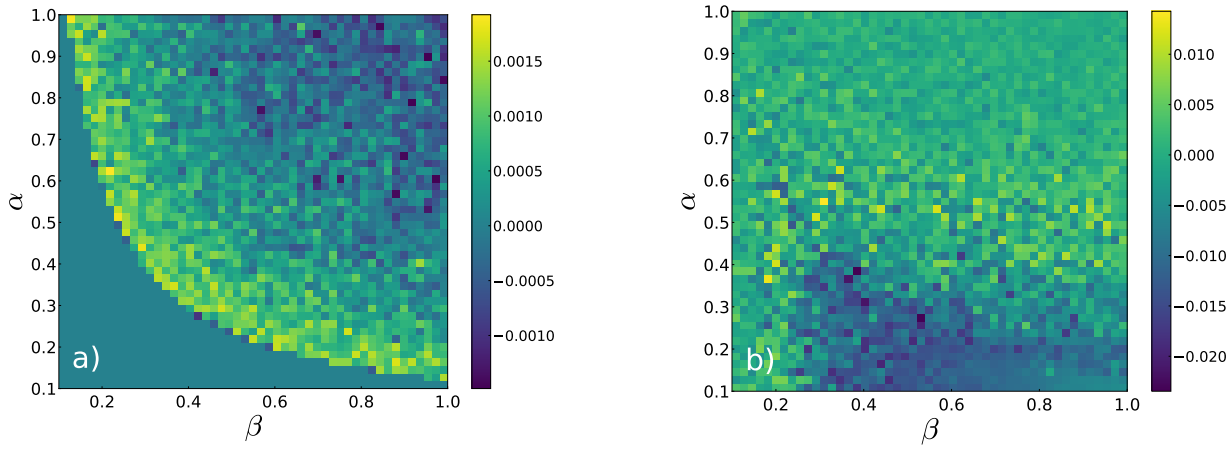

FIG. S3. Difference between the quantities computed using Monte Carlo simulations and their analytical counterparts for various values of parameters α and β. Panel a (b) presents the case of y_{eq} The other parameters are set to $N = 1000$, $\gamma = 0.1$, $\mu = 0.2$, and $T = 1.0$, respectively.